Evaluation of Rainfall Forecasts over Taiwan by Four Cumulus Parameterization Schemes

Ming-Jen YANG

Institute of Hydrological Sciences, National Central University, Chung-Li, Taiwan ROC

and

Quen-Chi TUNG

Department of Atmospheric Sciences, Chinese Culture University, Taipei, Taiwan ROC

(Manuscript received 22 January 2003, in revised form 26 June 2003)

Abstract

This study compares rainfall forecasts by four cumulus parameterization schemes (CPSs), the Anthes-Kuo, Betts-Miller, Grell, and Kain-Fritsch schemes, using the fifth-generation Pennsylvania State University—National Center for Atmospheric Research Mesoscale Model (MM5) nesting down to 15-km grid spacing. Six rainfall events over the Taiwan area are selected to investigate the CPS performance. The precipitation forecast is evaluated over the model grid points using statistical scores (threat score, equitable threat score, and bias score) for different threshold values based on island-wide rain gauge observations.

The results show that except for the warm-season events (spring rainfall and summer thunderstorm cases), the 15-km MM5, using any of the four CPSs, shows good skill for predicted coverage of measurable 6-h rainfall over the Taiwan area. For rainfall-area and rainfall-amount predictions, the model performs better in cold-season events (winter cold-air outbreak and autumn cold front cases) than in warm-season events, in agreement with previous studies. None of these CPSs consistently outperforms the others in all measurements of forecast skill, and each CPS performs very differently for precipitation prediction under different synoptic forcings. For precipitation events with strong synoptic-scale forcings (like the winter cold-air outbreak and Mei-Yu front cases), the synoptic forcing and Taiwan's topography provide the primary control on the model's rainfall forecast, and the CPSs used in the model only modify precipitation prediction slightly.

In the wettest 3 of 6 cases, the ensemble prediction with an arithmetic average of rainfall forecasts by four CPSs has the best threat score at 0.25-mm threshold. The 15-km MM5 generally overpredicts the area of light rainfall, and underpredicts the area of heavy rainfall, and the model tends to have better predictive skill in the lower land than over the mountainous area in Taiwan. Except for the spring rainfall case, all CPSs underestimate precipitation amount, especially for heavy rainfall cases (Mei-Yu front and Typhoon Otto). The Grell experiment has the best skill in total accumulated rainfall prediction in four out of six cases; the Betts-Miller experiment has the best performance for the rainfall maximum forecast in three out of six cases.

The characteristic responses of four CPS experiments over the Taiwan area are: (i) Anthes-Kuo experiment tends to overpredict the rainfall area, especially for light precipitation events; (ii) Betts-Miller

Corresponding author: Ming-Jen Yang, Institute of Hydrological Sciences, National Central University, 300 Chung-Da Road, Chung-Li, Taiwan 320, R.O.C.
E-mail: mingjen@cc.ncu.edu.tw

experiment is inclined to produce heavy rainfall, and it underpredicts the rainfall area; (iii) Kain-Fritsch experiment has the best skill in rainfall-area prediction for the winter cold-air outbreak case; and (iv) Grell experiment has the best predictive skill for the heavy-rainfall events of the Mei-Yu front, and Typhoon Otto cases.

1. Introduction

Many cumulus parameterization schemes (CPSs) have been developed and implemented in numerical weather prediction models. However, most CPSs are developed in specific convective environments, and are evaluated in a limited number of cases (Kuo et al. 1996; Wang and Seaman 1997; Peng and Tsuboki 1997; Yang et al. 2000). None of the CPSs are systematically evaluated for precipitation systems in a subtropical environment with pronounced orography, such as the Taiwan area. Therefore, this study compares rainfall forecasts by a few CPSs for precipitating events in the Taiwan area.

Wang and Seaman (1997) performed a comparison study of four CPSs, the Anthes-Kuo (AK; Anthes 1977), Betts-Miller (BM; Betts and Miller 1986), Grell (GR; Grell 1993), and Kain-Fritsch schemes (KF; Kain and Fritsch 1993), using the fifth-generation Pennsylvania State University—National Center for Atmospheric Research Mesoscale Model (MM5). Performance of these CPSs was examined using six precipitation events over the continental United States for both cold and warm seasons. They found that no one CPS always outperformed the others. The general 6-h precipitation forecast skill for these schemes was fairly good in predicting four out of six cases examined in the study, even for higher precipitation thresholds. The forecast skill was generally higher for cold-season events than for warm-season events. The model's precipitation skill is better in rainfall volume than in either areal coverage or peak amount. In this study, the work of Wang and Seaman (1997) will be extended to a subtropical setting in Taiwan.

Du et al. (1997) showed that short-range ensemble forecasts have some increased skill in precipitation prediction in comparison to a single high-resolution forecast. However, the tendency for ensemble averaging, with a smoothing nature, may be detrimental to other aspects (like intensity and maximum) of the rainfall forecast. The practical advantage of precipitation prediction by ensemble forecasting, with a mixture of cumulus parameterizations, deserves more investigation. In addition, the ensemble forecast is still limited by the accuracy of the model and analysis used.

The research purposes of this study are threefold. First, do CPSs have consistent and systematic performance in different synoptic environments? Second, what is the general applicability of CPSs when they are applied in the Taiwan area rather than in those original environments tested by the developers? Third, can a precipitation prediction based on an ensemble of CPSs provide a better forecast than that by one single CPS?

This study follows Wang and Seaman (1997), and Yang et al. (2000) to evaluate the performance of four CPSs in fully prognostic tests, using six rainfall events in four seasons over the Taiwan area. *Categorical statistics scores* and *rainfall amounts* over 6-h periods are evaluated for each CPS experiment. The mesoscale model used is the Penn State/NCAR MM5 model at grid sizes of 45 and 15 km. These horizontal resolutions are similar to those of the operational regional model used in Taiwan (by the Central Weather Bureau) recently. Each precipitation forecast is evaluated statistically over 15-km grid points over Taiwan, using conventional skill scores for different precipitation threshold values.

One of the goals of this study is not only to understand the performance of CPSs on precipitation forecasts for a given case, but also to investigate differences in precipitation forecasts of a given CPS under different synoptic conditions. The limited sample size (four CPSs for six cases) will probably put some constraints on comparison results; however, the systematic comparison of these experiments should yield some useful information that can assist forecasters in Taiwan for rainfall predictions.

2. Methodology

2.1 Model and experiment design

The nonhydrostatic version of MM5 (Grell et al. 1994; version 2.11) is used as a common

testing framework to investigate rainfall forecasts of four CPSs. Other important physical parameterizations used in MM5 include the "simple ice" microphysics scheme (Dudhia 1989), the Blackadar (1979) planetary boundary layer scheme (Zhang and Anthes 1982), and a radiation scheme with interaction between clear sky and clouds (Dudhia 1989).

Following Kuo et al. (1996) and Wang and Seaman (1997), four CPSs chosen for evaluation in this study are the Anthes-Kuo scheme (AK), the Betts-Miller scheme (BM), the Grell scheme (GR), and the Kain-Fritsch scheme (KF). Descriptions of these CPSs can be found in referenced papers, and also in Kuo et al. (1996) and Wang and Seaman (1997).

Five numerical experiments are conducted for each precipitation case. These five experiments include four in which each simulation with a different CPS (AK, BM, GR, or KF) represents one rainfall forecast experiment. In order to explore the potential of an ensemble forecast, with a mixture of different CPSs, an average forecast (AF) is also made by arithmetically averaging the rainfall forecasts by the four CPSs. All parameters in the CPSs remain constant among simulations for different cases, in a manner similar to an operational setting.

The MM5 configuration includes a coarse mesh of 45-km grid size, and a fine mesh of 15-km grid size (Fig. 1). The 45-km domain has 81×71 grid points, and the 15-km domain has 91×91 grid points, with 27 σ levels in the vertical for both domains. Each MM5 run is 36 hours. In order to mimic the operational setting over Taiwan where the Central Weather Bureau has a global spectral model (the Central Weather Bureau Global Forecast System; CWBGFS, Liou et al. 1997), the initial conditions for each MM5 run are provided by the CWBGFS analysis field, and boundary conditions are provided by the CWBGFS forecast field. Routine surface observations, and sounding data, are included through the MM5 objective analysis package (RAWINS) to improve the initial condition field.

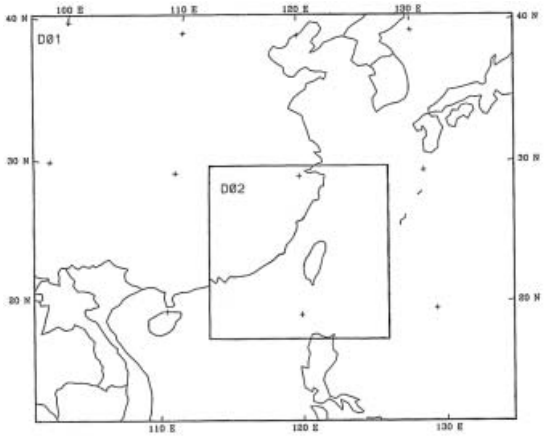

Fig. 1. Computational domains for the 45-km and 15-km grid sizes.

2.2 *Rainfall dataset*

The observations used to evaluate MM5 rainfall predictions are the rainfall data collected by the automatic rain gauge stations at the Central Weather Bureau in Taiwan. This data set consists of 343 rain gauge stations around Taiwan, with an average station spacing less than 5 km (see Fig. 2). The observed rainfall data are then interpolated to the 15-km model

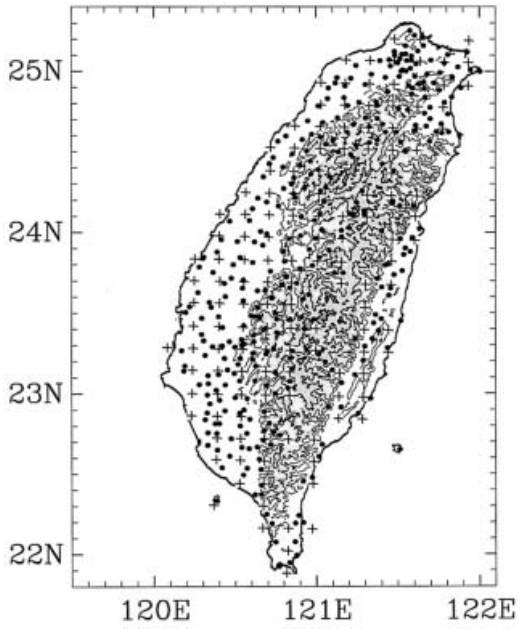

Fig. 2. Rain gauge stations (small dots) and the 15-km model grid points (crosses) over the Taiwan area used in the evaluation of the cumulus schemes. Topographic contours are at 500, 1500, 2500, and 3500 m.

grid points (155 points available totally), using the Cressman (1959) objective analysis method. A radius of influence of 8.46 km around a grid point is used so that a circle with this radius covers the same area of a 15 km $\times$ 15 km grid square, assuming that the simulated rainfall on a 15-km grid point represents the area-averaged rainfall over that grid square. If there is no rain gauge station around a grid point within the distance of one radius of influence, then that grid point is not used for rainfall verification. Averaging rainfall data arithmetically inside the circle area with one radius of influence (a method commonly used in operational centers like NCEP) is also tested; the evaluation results (not shown) are very similar to those to be discussed in Section 4, and only slight differences are found for the light rainfall events during the warm seasons.

2.3 Verification

The model prognostic fields (rainfall distribution, sea level pressure, and wind) are first verified against satellite imagery and objective analyses, to make sure that the model has adequate skill to reproduce the synoptic-scale features with embedded mesoscale precipitating systems. Then, the categorical statistics scores (Hamill 1999; McBride and Ebert 2000) such as threat score (TS), equitable threat score (ETS), and bias score (BS) are evaluated for several threshold values (0.25, 2.5, 10, 15, 20, and 25 mm), based on the 6-h rainfall forecast by each CPS experiment on the 15-km grid points. The reason for evaluation of the rainfall forecast over the model grid points in this study, not over the surface or rain gauge stations as in Mesinger (1998) and Colle et al. (1999), is because the evaluation area (Taiwan island) has more rain gauge stations than model grid points to perform objective analysis (see Fig. 2). Note that total (both parameterized and resolved) precipitation is evaluated. Because there are only a few 45-km grid points in Taiwan (17 points totally), categorical statistics scores with such a limited sampling of points probably do not have much statistical meaning; thus the 45-km verification results over the Taiwan area are not discussed.

For precipitation amount forecasting, the following statistical parameters are examined: mean error, mean error percentage, precipitation summary percentage, and precipitation maximum percentage. Definitions, and descriptions of the categorical statistical scores, and rainfall-amount parameters, are given in the Appendix.

3. Precipitation cases

Six cases are selected to represent a variety of synoptic and mesoscale weather conditions producing rainfall over the Taiwan area. Two cold-season cases, two warm-season cases, one Mei-Yu front case, and one typhoon case are selected. Table 1 lists the case number, the period of simulation, the type of synoptic environment, the duration of precipitation, and the maximum 36-h rainfall (after objective analysis) for each case.

Table 1. Summary of precipitation events.

Case	Period	Synoptics	Precipitation period	Max. 36-h rainfall (mm)
1	0000 UTC 18 Feb.–1200 UTC 19 Feb. 1999	Spring rainfall	0600 UTC 18 Feb.–1200 UTC 19 Feb. 1999	28.9
2	1200 UTC 27 Aug.–0000 UTC 29 Aug. 1998	Summer thunderstorm	Entire period	102.2
3	0000 UTC 6 Oct.–1200 UTC 7 Oct. 1998	Autumn cold front	Entire period	163.3
4	0000 UTC 11 Jan.–1200 UTC 12 Jan. 1999	Winter cold-air outbreak	Entire period	74.2
5	0000 UTC 27 May–1200 UTC 28 May 1999	Mei-Yu front	Entire period	283.7
6	0000 UTC 4 Aug.–1200 UTC 5 Aug. 1998	Typhoon Otto	Entire period	315.2

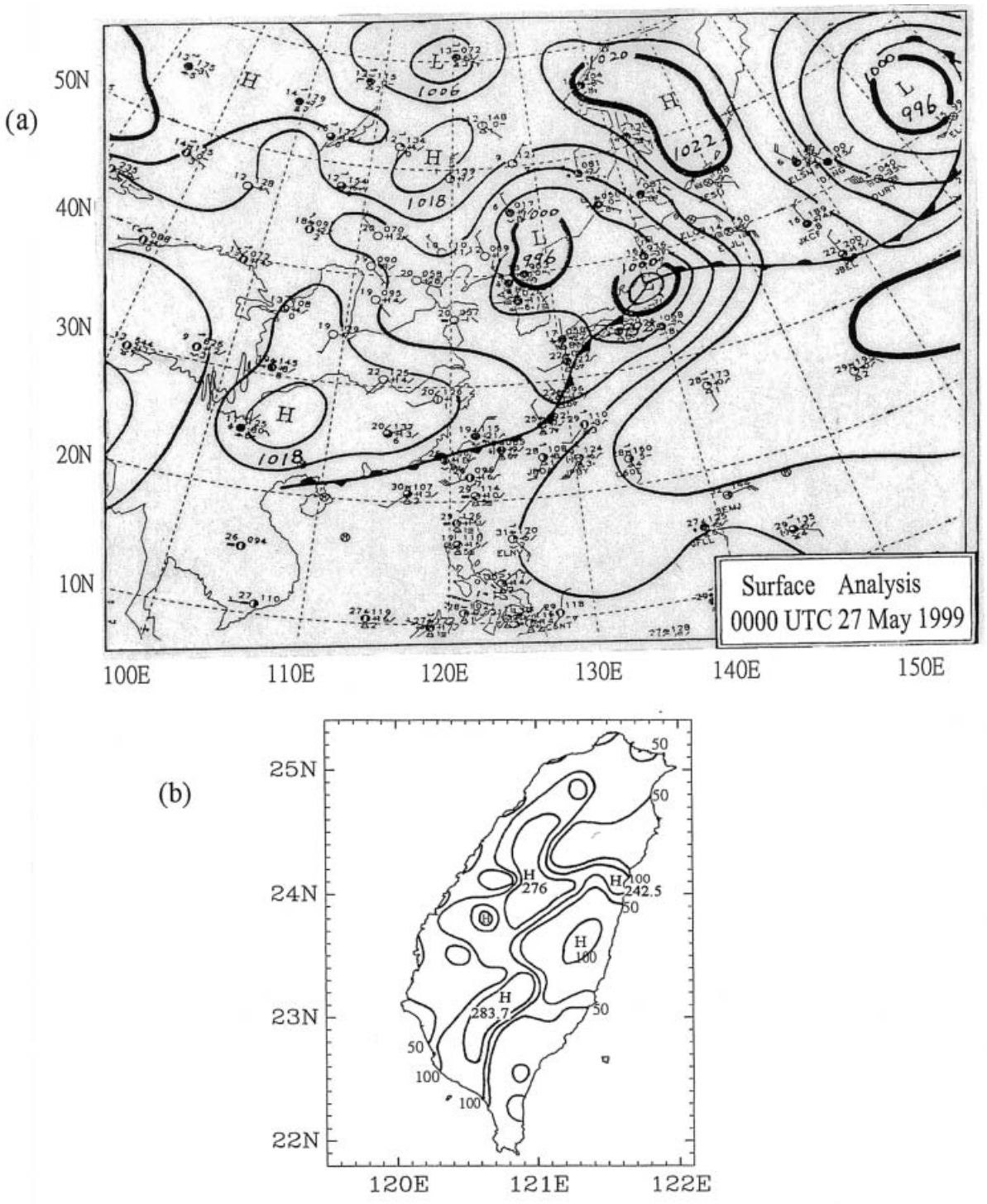

Fig. 3. (a) Surface analysis at 0000 UTC 27 May 1999 and (b) 36-h accumulated rainfall (in units of mm) over Taiwan from 0000 UTC 27 May to 1200 UTC 28 May 1999. Abbreviated plotting symbols in (a) follow usual convention with wind in knots (full barb, 10 knots), pressure and pressure tendency in hPa (ten and unit digits), temperature in degrees Celsius, and 6-h precipitation in mm; isobars are in solid lines (with contours of 4 hPa). Accumulated rainfall in (b) is contoured at 50, 100, 150, 200, and 280 mm.

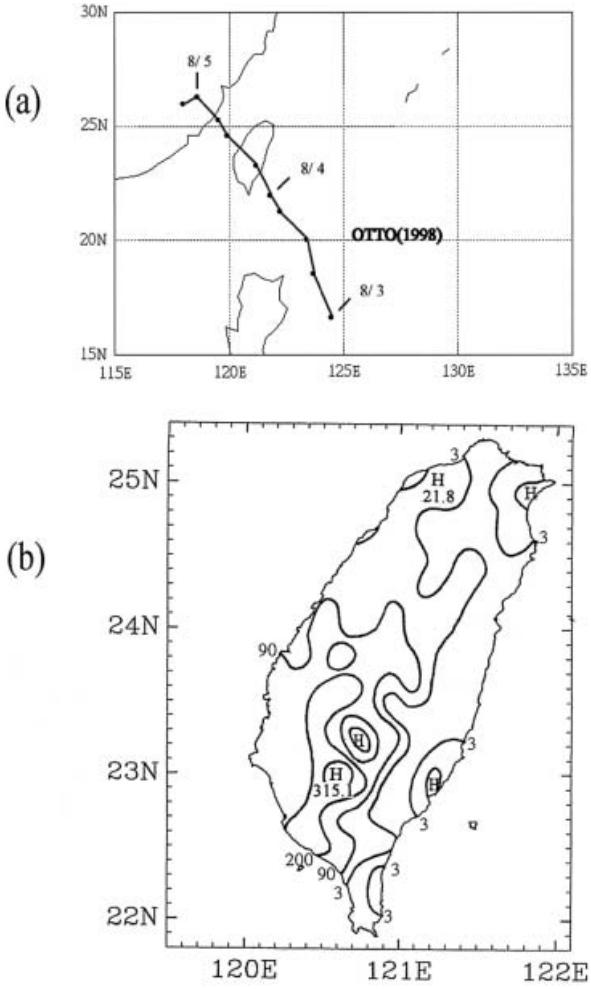

Fig. 4. (a) Bets track of Typhoon Otto and (b) 36-h accumulated rainfall (in units of mm) over Taiwan from 0000 UTC 4 August to 1200 UTC 5 August 1999. Dots along the best track in (a) represent the positions of typhoon center every 6 hours. Accumulated rainfall in (b) is contoured at 3, 90, 200, and 300 mm.

A Mei-Yu front (or Baiu front in Japan) on 27 May 1999, and the Typhoon Otto (1998) case, were chosen to represent the Mei-Yu front and typhoon cases which produced the most intense rainfall over the Taiwan area (see the max. 36-h rainfall in Table 1). The surface analysis at 0000 UTC 27 May 1999 is shown in Fig. 3a. A quasi-stationary Mei-Yu front extended from Japan to Taiwan to southern China. Ahead of the front, the wind was mainly southwesterly; behind the front, the wind varied from northeasterly to northerly. There were several mesoscale convective systems associated with this Mei-Yu front, resulting in heavy rainfall over the entire Taiwan island (Fig. 3b). The northwestward track of Typhoon Otto is shown in Fig. 4a. Once Typhoon Otto hit the Central Mountain Range in Taiwan, its intensity weakened quickly and it became a tropical storm after making landfall over China. Because of abundant moisture associated with the typhoon's southwesterly flow impinging on the Central Mountain Range after Otto left Taiwan, there was a lot of rainfall and flooding in the western and southern Taiwan (Fig. 4b). The horizontal distribution of 36-h accumulated rainfall for the other 4 cases is shown in Fig. 5, which will be discussed in a later section.

The synoptic-scale environments for the cold-season events were characterized by a wintertime cold-air outbreak and an autumn cold front. For the cold-air outbreak case, a strong high-pressure system originated over Mongolia and northern China moved southeastward, and then the Taiwan island was dominated by its associated cold-air mass (Fig. 6). Most of precipitation occurred on the windward slopes in northeastern Taiwan (Fig. 5a). This synoptic condition, and the associated rainfall pattern, are quite common during wintertime cold-air outbreaks in Taiwan. For the autumn cold front case, a cold front was from southern Japan to central Taiwan, and its rainfall was mainly over the eastern and southern Taiwan (Fig. 5b).

The synoptic-scale conditions for the warm-season cases were associated with spring-season frontal rainfall and summertime afternoon thunderstorms. For the spring rainfall case, a weak cold front was from southern Japan to southern China; the atmospheric conditions over the Taiwan area became unstable with the approaching of a weak cold front, and there was some sporadic rainfall on the eastern mountain slope (Fig. 5c). For the summertime thunderstorm case, a cold front was from Japan, eastern China Sea, to southern China; the wind around the Taiwan area was southwesterly and westerly. Precipitation over northern Taiwan was associated with frontal convection, and rainfall over southwestern Taiwan was

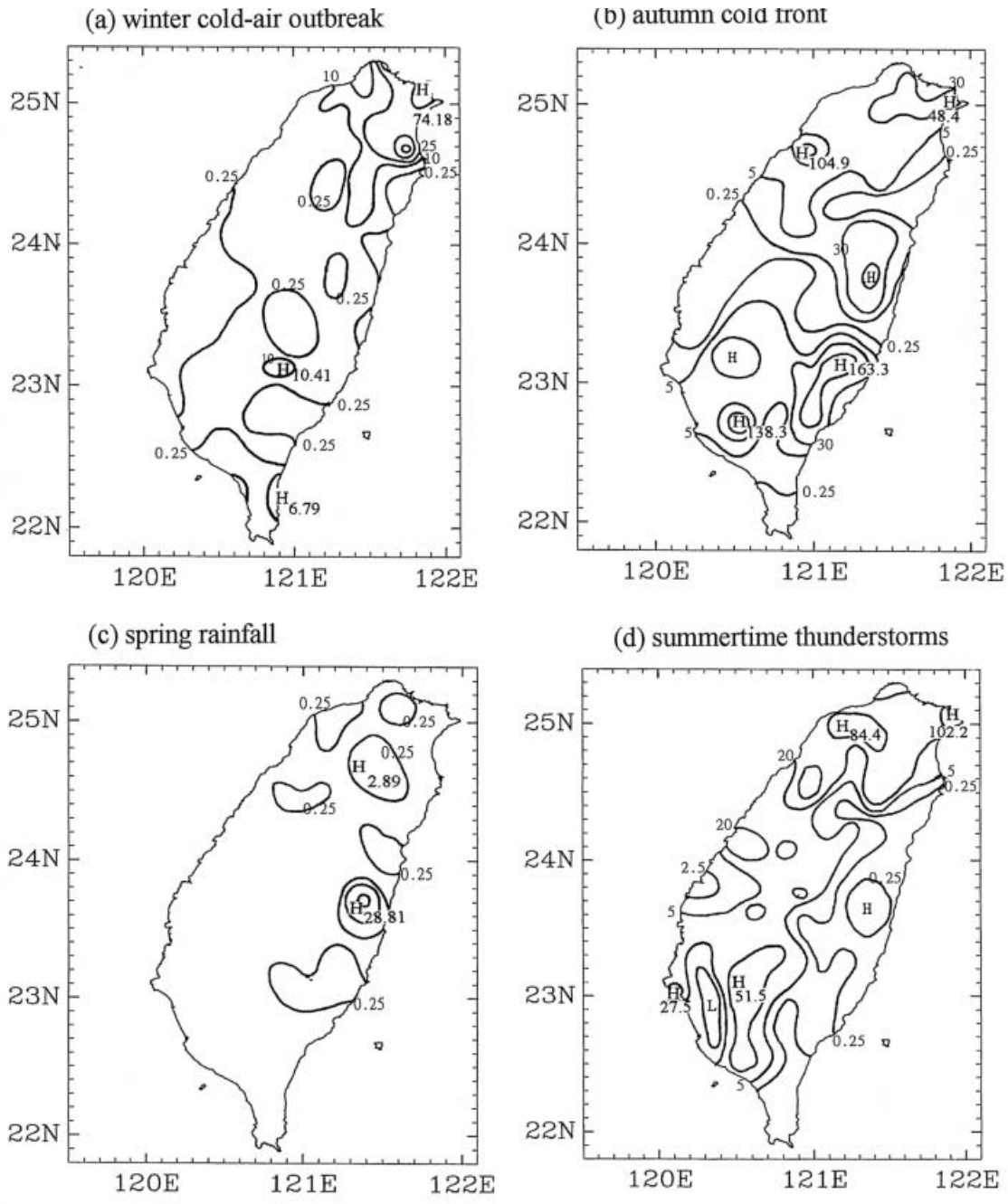

Fig. 5. 36-h accumulated rainfall (in units of mm) for (a) winter cold-air outbreak case (0000 UTC 11 January to 1200 UTC 12 January 1999), (b) autumn cold front case (0000 UTC 6 October to 1200 UTC 7 October 1998), (c) spring rainfall case (0000 UTC 18 February to 1200 UTC 19 February 1999), and (d) summertime thunderstorms case (1200 UTC 27 August to 0000 UTC 29 August 1998). Rainfall in (a) is contoured at 0.25, 10, 25, 40, and 70 mm; rainfall in (b) is contoured at 0.25, 5, 30, 75, and 160 mm; rainfall in (c) is contoured at 0.25, 10, and 25 mm; rainfall in (d) is contoured at 0.25, 5, 20, 50, and 100 mm.

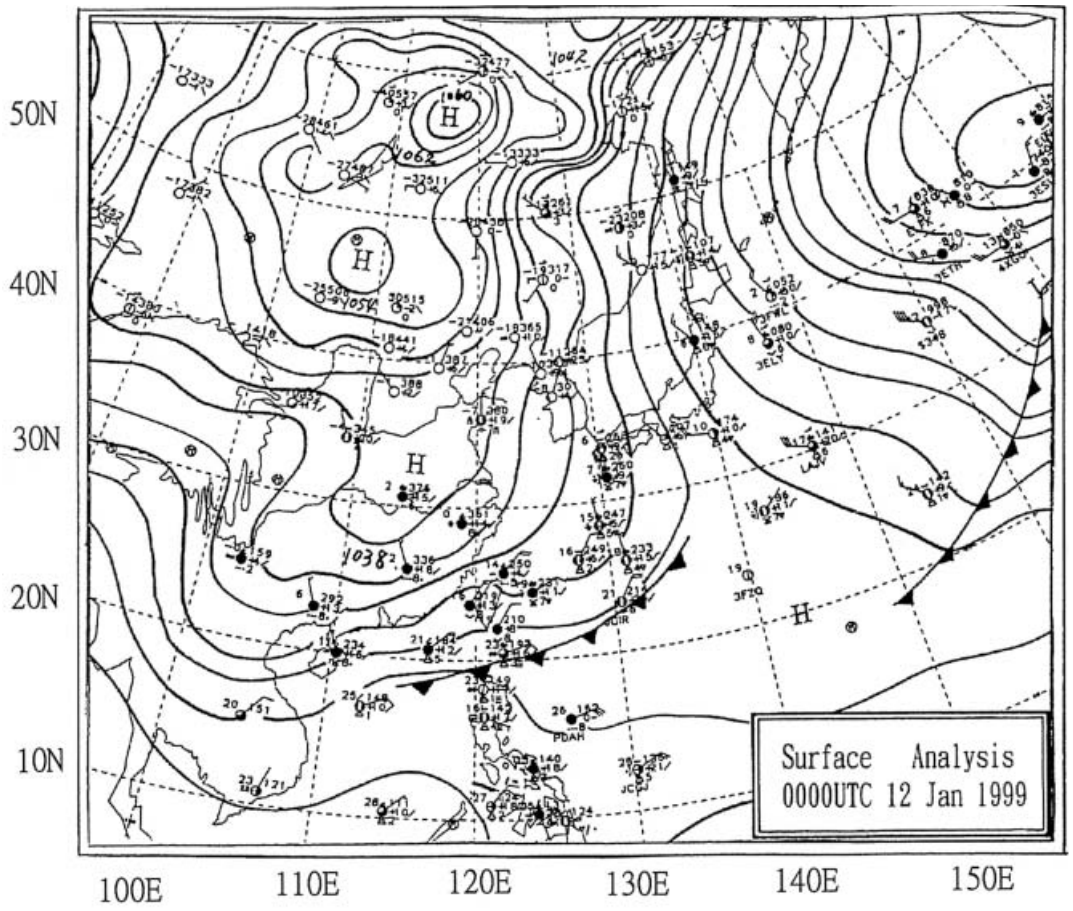

Fig. 6. Surface analysis at 0000 UTC 12 January 1999. Isobars are in solid lines (with contours of 4 hPa). Abbreviated plotting symbols are same as in Fig. 3a.

produced by orographic lifting of warm air from the South China Sea (Fig. 5d).

4. Results

4.1 Prediction of synoptic-scale features

Verification of the simulated rainfall distribution, sea-level pressure, and wind fields of six rainfall cases, with satellite pictures and observational analyses, indicates that simulations with different CPSs do not have evident differences in the synoptic-scale features. This implies that simulations of large-scale (and/or synoptic-scale) features are not sensitive to the CPSs used in the model (Kuo et al. 1996; Wang and Seaman 1997; Peng and Tsuboki 1997). To show an example, Fig. 6 is the surface analysis of the winter cold-air outbreak case and Fig. 7

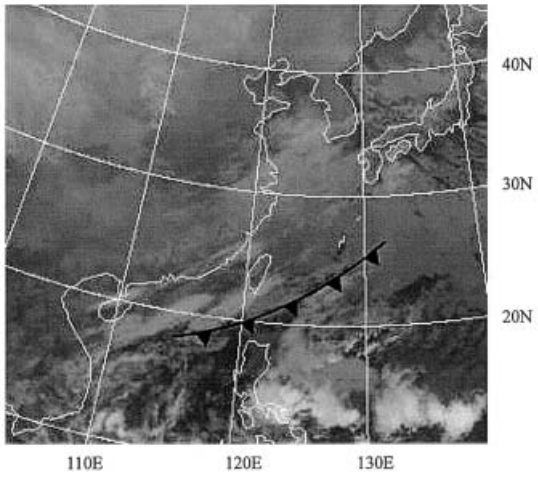

Fig. 7. IR satellite picture at 0000 UTC 12 January 1999. The cold-air boundary is indicated by the cold-front symbol.

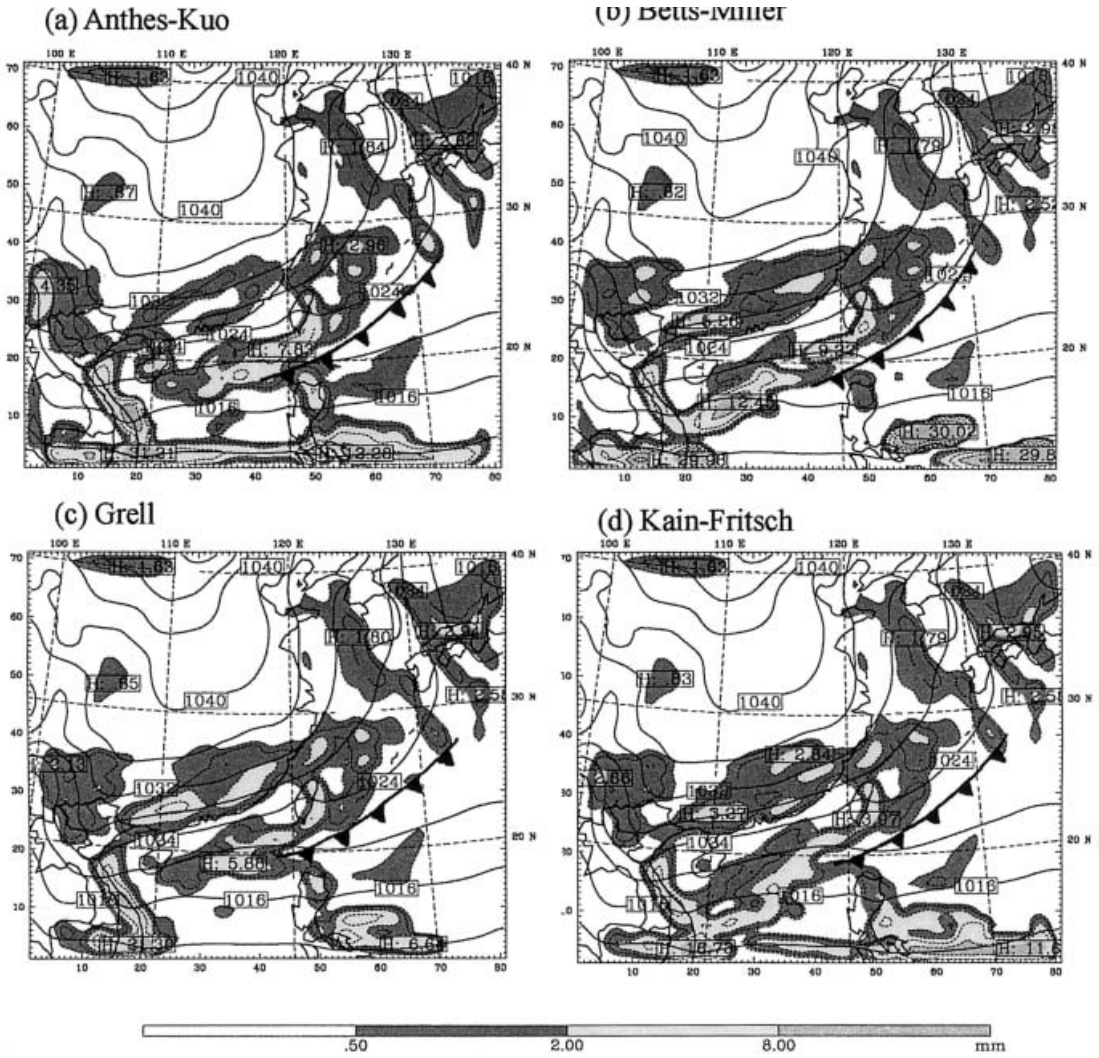

Fig. 8. Simulated sea-level pressure with contours of 4 hPa for various cumulus parameterizations on the 45-km grid at 24 hours into the simulation (valid at 0000 UTC 12 January 1999): (a) Anthes-Kuo, (b) Betts-Miller, (c) Grell, and (d) Kain-Fritsch schemes. Shading indicates 6-hourly (1800 UTC 11 January to 0000 UTC 12 January) accumulated rainfall in units of mm. The cold-front symbol indicates the cold-air boundary.

is the corresponding satellite image. Figure 8 further shows the simulated sea-level pressure and 6-h accumulated rainfall by four CPSs on the 45-km grid for this event. The cold-air outflow boundary is also indicated in Figs. 6, 7, and 8. It is clear from Fig. 8 that despite using different CPS, each experiment produced a similar sea-level pressure field, which was in close agreement with observations (Fig. 6). The simulated precipitation distribution on this scale (45-km grid size) still showed strong resemblance to each other, although the intensity and detailed structure had appreciable differences among these experiments.

4.2 Categorical statistics scores

Let us first discuss the threat scores for all six events. Figure 9 shows threat scores (TSs) at the 0.25-mm threshold for 6-h rainfall predictions. It is shown that except for two warm-season events (spring rainfall and summertime thunderstorm cases), the 15-km MM5 using four CPSs generally shows good predictive skill for coverage of measureable 6-h rainfall

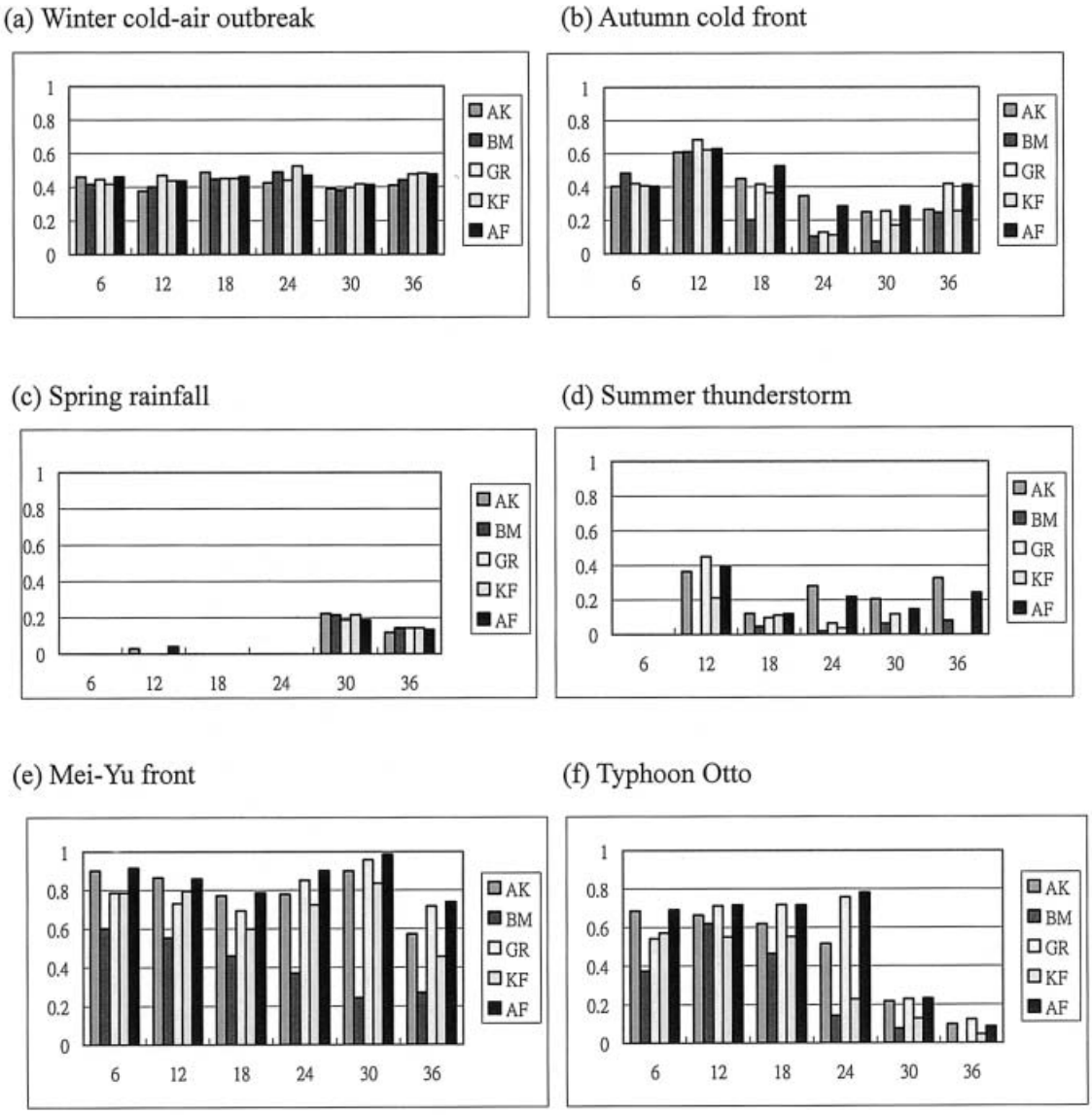

Fig. 9. Threat scores (TSs) at the 0.25-mm threshold for 6-h rainfall predictions from 15-km MM5 runs for the (a) winter cold-air outbreak, (b) autumn cold front, (c) spring rainfall, (d) summer thunderstorm, (e) Mei-Yu front, and (f) Typhoon Otto case. The times on the abscissa are relative to the model's initial time.

for four precipitation cases over the Taiwan area, with TSs greater than 0.4 at the precipitation threshold of 0.25 mm. Because the forcing mechanisms for warm-season rainfall are on small scale, not on synoptic scale, models usually have less skill at predicting warm-season rainfall. The model did poorly for the spring-season frontal rainfall case (Fig. 9c), and the timing error of the frontal movement (slower by 6～12 h) might cause such bad rainfall forecasts. Because summertime precipitation was mainly generated by thermal forcing and topographic lifting, which the 15-km MM5 could not adequately represent with such a coarse horizontal resolution, the model had poor TS performance (Fig. 9d). For the Mei-Yu front case (Fig. 9e), the TSs for most experiments (except for BM) were above 0.57, with

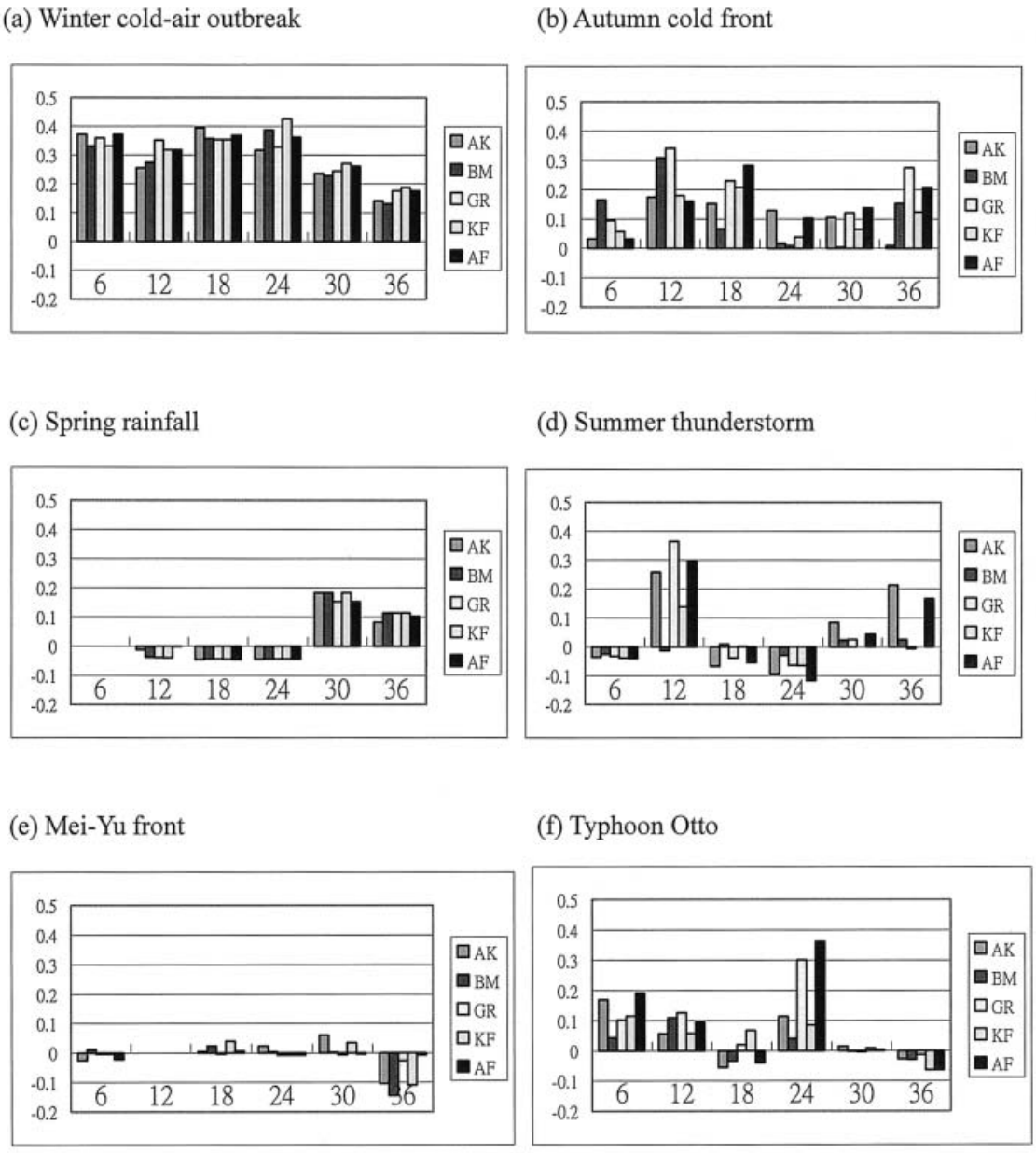

Fig. 10. As in Fig. 9 but for the equitable threat score (ETS).

the highest TS of 0.99 by AF at hour 30. For Typhoon Otto case (Fig. 9f), all experiments had good TSs (0.4 ~ 0.8) in the first 18 hours; after hour 24, the predicted typhoon track started to deviate appreciably from the observed track (24-h track error is about 150 km), and the TSs of all experiments dropped significantly.

Figure 10 further shows equitable threat scores (ETSs) at the 0.25-mm threshold for 6-h rainfall predictions. For two cold-season events (Figs. 10a and 10b), the 15-km MM5 had a pretty good prediction scores, compared to their warm-season counterparts (spring rainfall and summertime thunderstorm; Figs. 10c and 10d). The ETS scores for Mei-Yu front event (Fig. 10e) are near or below zero, indicating basically no predictive skill for 6-h rainfall of this Mei-

Table 2a. Equitable threat scores averaged over six 6-h periods for different precipitation thresholds of two cold-season cases. Threshold is in units of mm. The score with an asterisk is the best forecast at a given precipitation threshold.

Threshold	AK	BM	GR	KF	AF
0.25	0.1933	0.2020	0.2404*	0.2132	0.2318
2.5	0.1984*	0.1703	0.1860	0.1603	0.1769
5	0.1241*	0.0880	0.0974	0.0928	0.1008
10	0.0366*	0.0210	0.0116	0.0213	0.0186
15	0.0212*	0.0169	0.0081	0.0134	0.0201
20	0.0186*	0.0075	−0.0031	0.0019	−0.0051
25	0.0026	0.0109*	−0.0038	−0.0031	−0.0028

Table 2b. As in Table 2a but for the bias scores.

Threshold	AK	BM	GR	KF	AF
0.25	1.3214	0.9393	1.1066	1.0416*	1.2959
2.5	1.0210*	0.7887	0.8328	0.8197	0.8958
5	0.7918*	0.6971	0.6941	0.5312	0.6153
10	0.4312	0.7190*	0.6811	0.4953	0.5928
15	0.1652	0.3787*	0.3696	0.2020	0.3457
20	0.1686	0.4473*	0.4145	0.2677	0.2714
25	0.1153	0.5639*	0.3333	0.2813	0.1875

Yu front event. Because of the quasi-stationary nature of the Mei-Yu front, there was rainfall almost over the whole island for this case (see Fig. 3b). Thus the number of successful hits (H in Appendix) is close to the number of hits by random guess (E in Appendix), resulting in near zero ETSs [see (A2) in Appendix for the definition of ETS]. For the Typhoon Otto case (Fig. 10f), all experiments lost their rainfall predictive skill after 24 hours. It is because of the large 24-h typhoon track error, resulting in zero or negative ETSs.

Table 2 is the ETS and BS averaged over six 6-h periods at different thresholds for two cold-season cases. Table 2a indicates that for cold-season events, the ETSs of all experiments were very similar (around 0.2 at 0.25-mm threshold). For precipitation thresholds of 15 mm and above, all experiments with near zero or negative ETSs showed little predictive skill, consistent with the findings of Stensrud et al. (2000) and Gallus and Segal (2001) that models with grid sizes of 10–25 km have little skill for 6-h rainfall amounts of 12.5 mm or above. Table 2b further indicates that the MM5 generally overpredicted the lightest rainfall (with BSs more than one at 0.25-mm threshold), and underpredicted medium-to-heavy rainfall (with BSs less than one for thresholds of 5 mm and above).

Table 3a indicates that for warm-season cases, all experiments had very low averaged ETSs, compared to those for cold-season cases. Table 3b further shows that all experiments had overforecasting at light-rainfall thresholds (0.25–2.5 mm), with BSs greater than one.

Since for this quasi-stationary Mei-Yu front case, the number of successful hits is close to the number of hits by random guess, the ETSs averaged in six 6-h periods are near or below zero for all five experiments (Table 4a). Table 4b shows that all experiments underforecasted occurrence of Mei-Yu frontal rainfall (with BS less than one) for all precipitation thresholds; in particular, BM had a consistent underforecasting of Mei-Yu frontal rainfall for all thresholds.

For the Typhoon Otto case, Table 5a indicates that the ETSs averaged in six 6-h periods were very low for all experiments, especially for heavy rainfall amounts (ETS less than 0.1 for 6-h rainfall of 15 mm and higher). Table 5b then shows that BM persistently underfore-

Table 3a. As in Table 2a but for two warm-season cases.

Threshold	AK	BM	GR	KF	AF
0.25	0.0434*	0.0136	0.0324	0.0173	0.0385
2.5	0.0219*	0.0022	0.0015	0.0067	0.0107
5	−0.0019	0.0095	0.0026	0.0206*	−0.0049
10	−0.0019	−0.0005	0.0054*	−0.0030	0.0002
15	−0.0018	0.0011*	−0.0011	−0.0003	−0.0005
20	−0.0004	0.0020*	0	0	0
25	0	−0.0004	0	0	0

Table 3b. As in Table 2b but for two warm-season cases.

Threshold	AK	BM	GR	KF	AF
0.25	2.5741	1.3106*	1.6404	1.6931	2.2839
2.5	3.5625	2.8084*	3.1161	3.4854	3.3426
5	1.8822	0.5922	0.8296	0.7846	0.8784*
10	0.6407*	0.1796	0.1324	0.2407	0.1777
15	0.4444*	0.0997	0.0163	0.0833	0.0139
20	0.0278	0.0308*	0	0	0
25	0	0.0417*	0	0	0

Table 4a. As in Table 2a but for the Mei-Yu front case.

Threshold	AK	BM	GR	KF	AF
0.25	0.0107	0.0070	−0.0033	0.0108*	−0.0042
2.5	0.0031	−0.0056	−0.0095	−0.0210	0.0119*
5	0.0043*	0.0038	−0.0229	−0.0465	−0.0198
10	−0.0050	0.0313*	−0.0242	−0.0399	−0.0298
15	−0.0272	0.0250*	−0.0345	−0.0397	−0.0411
20	−0.0197	0.0129*	−0.0225	−0.0266	−0.0084
25	−0.0072	−0.0044	0.0006*	−0.0215	−0.0119

Table 4b. As in Table 2b but for the Mei-Yu front case.

Threshold	AK	BM	GR	KF	AF
0.25	0.9057	0.4806	0.9088	0.7836	0.9884*
2.5	0.8067	0.3198	0.8246	0.6486	0.8917*
5	0.7449	0.2704	0.7942*	0.6126	0.7806
10	0.6849	0.2471	0.8592*	0.6704	0.6691
15	0.5468	0.1827	0.7747*	0.6619	0.4586
20	0.4407	0.1576	0.6691*	0.5552	0.2812
25	0.4618	0.1493	0.7791*	0.5856	0.2225

Table 5a. As in Table 2a but for the Typhoon Otto case.

Threshold	AK	BM	GR	KF	AF
0.25	0.0457	0.0215	0.0889	0.0451	0.0914*
2.5	0.0772	0.0447	0.1219*	0.0725	0.0988
5	0.0813	0.0373	0.1152*	0.0483	0.0797
10	0.0418	0.0069	0.0767*	0.0015	0.0456
15	0.0494	0.0028	0.0578*	0.0047	0.0244
20	0.0590*	0.0064	0.0584	0.0019	0.0217
25	0.0377	−0.0016	0.0398*	0.0033	0.0106

Table 5b. As in Table 2b but for the Typhoon Otto case.

Threshold	AK	BM	GR	KF	AF
0.25	1.1399*	0.4329	1.4128	0.6849	1.5104
2.5	1.0047*	0.4566	1.7232	0.6236	1.2211
5	0.7183	0.3777	1.5852	0.4999	0.8529*
10	0.7945*	0.1983	2.6987	0.1891	0.3099
15	0.4117*	0.1496	2.4022	0.0437	0.2181
20	0.1503	0.1322	1.6824*	0.0271	0.1138
25	0.1248	0.0945	0.4787*	0.0234	0.0842

casted the occurrence of typhoon rainfall for all thresholds.

4.3 Scores over mountain and lowland areas

Since Taiwan has substantial orography (see Fig. 2 for detailed terrain), it is interesting to know the difference in rainfall predictive scores, between mountain and lowland areas. Figure 11 shows the ETSs, and BSs for the winter cold-air outbreak case averaged for grid points, either in the lower land (terrain height below 500 m; 94 points totally), or over the mountainous area (terrain height above 500 m; 61 points totally). By comparing Figs. 11a and 11b, it is clear that after 18 hours of integration the 15-km MM5 had better ETSs in the lower land than over the mountain area. This indicates that a grid size of 15 km is probably not enough to fully resolve the topography-induced precipitation over the northeastern coastal terrain (see Fig. 5a for the horizontal distribution of 36-h accumulated rainfall for this case). For the simulated rainfall over the mountain area, the 15-km MM5 usually produces a broad smooth area of precipitation, but no detailed structure corresponding to fine-scale topography. The MM5, with 15-km horizontal resolution, was inclined to overforecast rainfall area over the mountain area (higher BSs in Fig. 11c), but the model mostly underforecasted or slightly overforecasted rainfall area in the plain area (lower BSs in Fig. 11d). Chien et al. (2002) also found that during the 1998 Mei-Yu season, the ETSs of 15-km MM5 over the Taiwan area were better in the lowlands than over the mountainous areas (slopes and highlands).

Because the Typhoon Otto case is the wettest and most severe case in six rainfall events examined in this study, it is also helpful to understand the influence of Taiwan's terrain on model's precipitation forecast skill. For this Typhoon Otto case, the 15-km MM5 again had better ETSs in the lower land than over the mountain area, especially at hours 12 and 24 (Figs. 12a and 12b). In the first 24 hours, the 15-km MM5 underforecasted or slightly overforecasted rainfall area both over the lower land and mountain area (BSs less than or slightly greater than one in Figs. 12c and 12d). After hour 24, when the typhoon track forecast error was large enough to substantially affect the rainfall predictions, the model strongly overforecasted rainfall area, especially in the lower land (Figs. 12c and 12d).

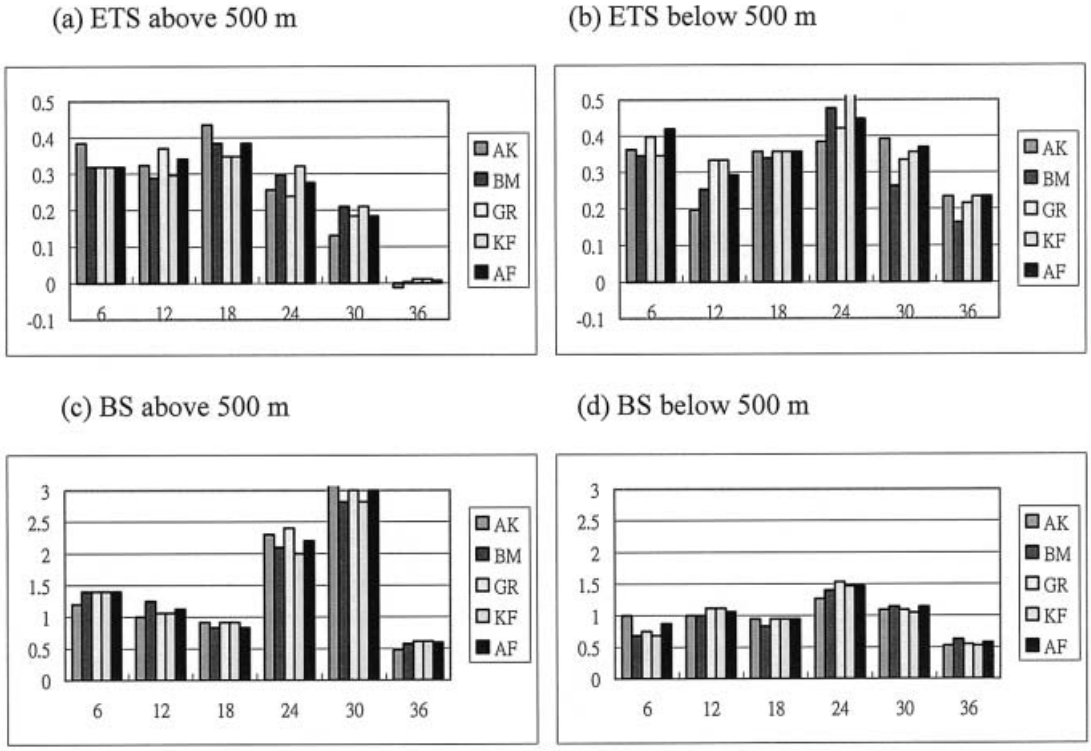

Fig. 11. Equitable threat score (ETS) and bias score (BS) averaged for grid points whose terrain heights are either above or below 500 m for the winter cold-air outbreak case. The ETS for grid points with terrain height above 500 m is in (a) and the ETS for grid points with terrain height below 500 m is in (b). The BS for grid points with terrain height above 500 m is in (c) and the BS for grid points with terrain height below 500 m is in (d). Threshold is 0.25 mm for 6-h rainfall predictions from five 15-km experiments. The times on the abscissa are relative to the model's initial time.

For this typhoon case, the BM experiment had a consistent underforecasting of the chance of rainfall, especially over the mountain area after 24 hours of integration (BS much less than one in Figure 12c). For the Betts-Miller (1986) scheme used in this study, the cloud depth must be greater than 290 hPa in order to trigger convection. This cloud depth may be too thick for mountain regions in Taiwan, and it may cause the BM experiment to have a consistent underforecasting. NCEP also had problems of the Betts-Miller-Janjic scheme (Janjic 1994) over the high-elevation areas in the Eta model (Baldwin et al. 2002).

The differences in ETSs and BSs over lowland and mountain areas for the other four cases are similar to those for the winter cold-air outbreak and Typhoon Otto case. Therefore for rainfall predictions in the Taiwan area, it is fair to say that *the 15-km MM5 generally had better ETSs over the lowland area than over the mountain area, and the MM5 underforecasted rainfall area over the lower land and overforecasted rainfall area over the mountainous region*.

4.4 Prediction skill for precipitation amount

Another important aspect of rainfall forecasting is the precipitation amount, which is the critical issue for quantitative precipitation forecasts (QPFs). Table 6a compares the mean errors (MEs) of 6-h rainfall amounts averaged over six 6-h periods for all experiments, and it shows negative MEs except for the spring rainfall event. This implies that with the exclusion of the spring rainfall case, the MM5 at 15-km grid underpredicted the 6-h precipitation amount for rainfall systems over Taiwan.

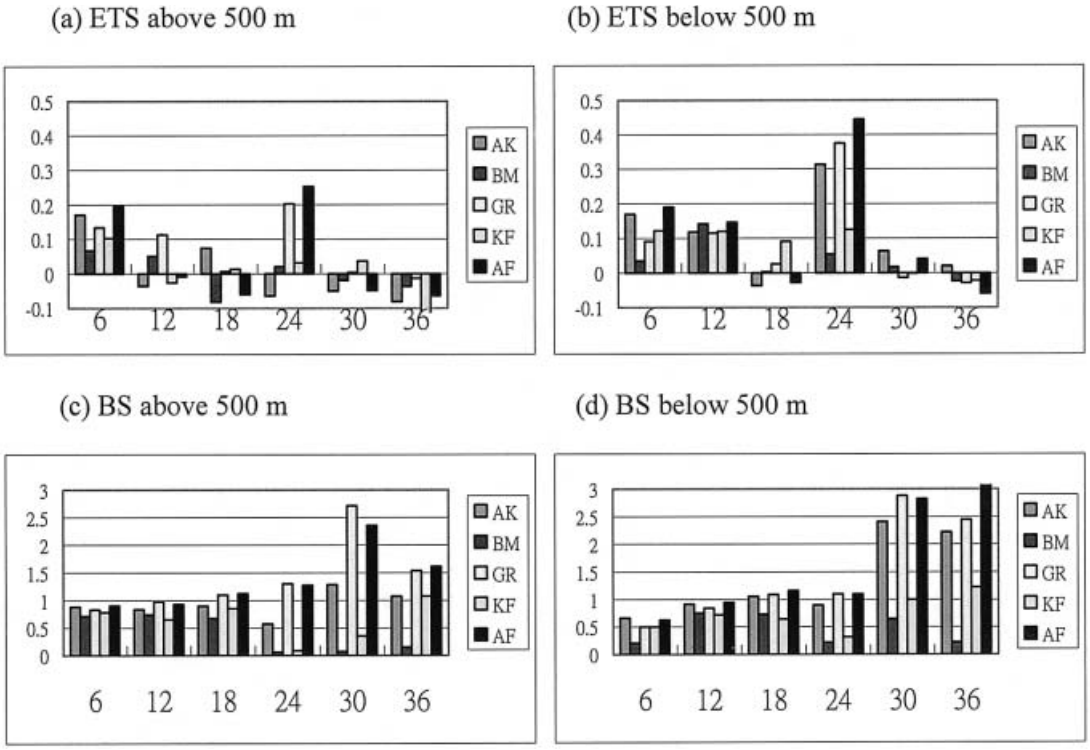

Fig. 12. As in Fig. 11 but for the Typhoon Otto case.

Table 6a. Mean errors (mm) for 6-h rainfall amounts averaged over six 6-h periods for five 15-km experiments. The number with an asterisk is the best forecast in a given case.

Case	AK	BM	GR	KF	AF
Spring rainfall	0.4782	0.2730	0.2585*	0.2808	0.3228
Summer thunderstorm	−2.1165*	−2.6517	−2.3992	−2.4310	−2.3995
Autumn cold front	−1.6218	−1.0438*	−1.3191	−1.4418	−1.3567
Winter cold-air outbreak	−0.3850	−0.3772	−0.3557*	−0.3837	−0.3753
Mei-Yu front	−8.7065	−14.7308	−8.1248*	−9.7403	−10.3257
Typhoon Otto	−12.1770	−12.3084	−7.1060*	−14.6754	−11.5666

To be specific, GR had the smallest ME in four out of six cases, including the heavy rainfall events with the Mei-Yu front and Typhoon Otto cases; AK had the lowest ME in the summertime thunderstorm event; BM had the lowest ME in the autumn cold front case.

Table 6b shows the mean error percentages (MEPs) for 6-h rainfall amounts averaged over six 6-h periods in all experiments, and it basically shows the same result as Table 6a. For the spring rainfall event, the 15-km MM5 severely overestimated the 6-h accumulated rainfalls, with MEPs between 240 and 440%. For other precipitation events, the model underestimated 6-h rainfalls with MEPs between −28 and −94%. If a fixed CPS is used to compare its performance under different synoptic environments, then it can be found from Table 6b that the MM5 had smaller MEPs in cold-season events than in warm-season events.

Table 6b. As in Table 6a but for the mean error percentage (%). The number with an asterisk is the best forecast in a given case and the number with a pound is the best forecast for a given cumulus experiment.

Case	AK	BM	GR	KF	AF
Spring rainfall	441.435	252.029	238.643*	259.260	298.034
Summer thunderstorm	−74.948*	−93.899	−84.957	−86.085	−84.969
Autumn cold front	−42.861	−27.586#*	−34.858	−38.104	−35.853
Winter cold-air outbreak	−35.846#	−35.117	−33.115#*	−35.722#	−34.946#
Mei-Yu front	−47.802	−80.877	−44.608*	−53.478	−56.691
Typhoon Otto	−71.082	−71.849	−41.481*	−85.666	−67.519

Table 7a. Precipitation summary percentages (%) of the 36-h periods for five 15-km experiments. The number with an asterisk is the best forecast in a given case and the number with a pound is the best forecast in a given cumulus experiment.

Case	AK	BM	GR	KF	AF
Spring rainfall	541.321	352.026	338.762*	359.235	397.844
Summer thunderstorm	25.055*	6.102	15.045	13.910	15.028
Autumn cold front	57.139	72.415*#	65.139	61.899	64.147
Winter cold-air outbreak	64.145#	64.881	66.874*#	64.285#	65.048#
Mei-Yu front	52.198	19.122	55.392*	46.522	43.308
Typhoon Otto	29.248	25.725	51.487*	13.804	30.066

Table 7b. As in Table 7a but for precipitation maximum percentages (%).

Case	AK	BM	GR	KF	AF
Spring rainfall	80.541*#	72.461	50.789	63.261	50.323
Summer thunderstorm	24.113	30.080*	16.861	13.859	19.237
Autumn cold front	25.081	81.101*	79.472#	54.040	47.461
Winter cold-air outbreak	60.633*	58.062	57.164	58.102	56.785
Mei-Yu front	56.962	48.993	54.897	64.582*#	49.972
Typhoon Otto	58.775	102.086*#	71.329	49.355	61.598#

Table 7a is the percentage of total precipitation amount (PSP) within the 36-h integration period for six events. Except for the spring rainfall case, the 15-km MM5 underpredicted total rainfall amount for all events, especially for the summertime thunderstorm case (with PSP of 6∼25%). For a given synoptic environment with different cumulus parameterizations, GR had the best forecast of total precipitation amount in four out of six cases; AK had the best forecast of total rainfall for the summertime thunderstorm event; BM had the best prediction of total rainfall for the autumn cold front case. On the other hand, for a given CPS applied in different synoptic environments, AK, GR, KF, and AF all had the best predictions for total precipitation amount for the winter cold-air outbreak case; BM had the best total-rainfall forecast for the autumn cold front event.

The precipitation maximum percentage (PMP) during the 36-h period is shown in Table 7b. The MM5 at 15-km grid underpredicted rainfall maxima for all events, especially for the summertime thunderstorm case (with PMP of 14∼30%). If we consider a given synoptic environment, and compare the predictions by different cumulus schemes, BM had the best forecast of precipitation maxima in three out of six cases; AK had the best forecast in two cases (spring rainfall and winter cold-air outbreak

cases); KF had the best prediction of rainfall maximum for the Mei-Yu front case.

5. Conclusions

Many studies have demonstrated that differences in cumulus parameterizations can have substantial impacts on simulated convection and precipitation (e.g., Rogers and Fritsch 1996; Gallus 1999). It is not the purpose of this study to judge one CPS as inherently better or worse than the other. Instead, four cumulus schemes are selected to demonstrate the variability in rainfall forecasts, both due to different cumulus parameterizations and various synoptic forcings, which will confront forecasters in their daily operation. The information obtained from these series of experiments should be useful for improvement of cumulus parameterization schemes intended for operational usage at a grid size of 15 km in a subtropical environment with substantial topography, or the Taiwan area in particular.

It is noted that precipitation prediction errors do not result only from a given CPS, but also may be related to deficiencies in other model physics, or to the coupling of a CPS with other model physics. Details in the model's initial conditions should also be important for obtaining a good rainfall forecast, especially for warm-season events when large-scale dynamical forcing is relatively weak. Statistical verification scores used in this study do not always provide a fully "objective" assessment of a rainfall forecast. Development of better evaluation methods for high-resolution nonhydrostatic models is greatly needed in the future.

With these limitations in mind, the principal findings, for the comparison of precipitation predictions by four cumulus parameterization schemes over the Taiwan area, are summarized below.

- For a precipitation event with strong synoptic-scale forcing (like the winter cold-air outbreak and Mei-Yu front cases), performance of each CPS is quite similar. On the other hand, for rainfall events with weak synoptic-scale forcings (like the spring rainfall and summertime thunderstorm cases), the difference of each CPS's performance can be quite large. This implies that the synoptic, or mesoscale environment, provides the primary control on the model's rainfall forecast skill, and the CPSs used in the model only slightly modify forecasts.
- Except for two warm-season events (spring rainfall and summertime thunderstorm cases), the 15-km MM5, using four CPSs, generally shows good predictive skill for coverage of measureable 6-h rainfall for four precipitation cases over the Taiwan area, with threat scores greater than 0.4 at the precipitation threshold of 0.25 mm.
- For rainfall predictions, the MM5 model performs better in cold-season events (winter cold-air outbreak and autumn cold front cases) than in warm-season events, in agreement with many previous studies (Wang and Seaman 1997; Gallus 1999).
- None of these CPSs consistently outperforms the others in all measurements of forecast skill, and each CPS has a very different performance for rainfall forecasting under different synoptic conditions (Wang and Seaman 1997).
- For the wettest 3 out of six cases, the ensemble forecast (AF experiment) with an arithmetic average of rainfall predictions by four CPSs has the best skill in predicting the occurrence of rainfall (i.e., the best threat score at 0.25-mm threshold). However, due to its inherent smoothing nature, the ensemble forecast only has moderate predictive skill in total precipitation amount and the peak rainfall intensity.
- In general, the 15-km MM5 tends to overpredict the area of light rainfall, and underpredict the area of heavy rainfall (Gallus 1999).
- The 15-km MM5 seems to have better predictive skill in the lower land than over the mountainous area, probably due to the fact that a grid size of 15 km is not enough to fully resolve the effects of Taiwan's topography on rainfall distribution and intensity.
- For the bias scores by four CPSs for the Mei-Yu front and Typhoon Otto cases in Taiwan, BM has a clear underforecasting. This is opposite to the finding that the Betts-Miller-Janjic scheme (Janjic 1994) in the NCEP Eta model has a relatively large overforecasting (Gallus 1999). It may be due to the various convection nature, and different geographical

location (subtropical oceanic environment versus midlatitude continental environment).

- Except for the spring rainfall case, all CPSs underestimate precipitation amount, especially for heavy rainfall cases (Mei-Yu front and Typhoon Otto), consistent with Spencer and Stensrud (1998) and Gallus (1999). For total rainfall amount prediction, GR has the best skill in four out of six cases. For the rainfall maximum forecast, BM has the best performance in three out of six events.
- The systematic behaviors of four CPS experiments for precipitating systems in the Taiwan area are listed here. AK experiment tends to overpredict the rainfall area, especially for light precipitation events. BM experiment is inclined to produce heavy precipitation in a localized area, and it underpredicts the rainfall area. KF has the best skill in rainfall-area prediction for the winter cold-air outbreak case. GR has the best predictive skill for the heavy-rainfall events of the Mei-Yu front and Typhoon Otto cases.

The large rainfall-forecast variability in these events raises concerns of relying upon one CPS for forecasting guidance. An approach to reduce this case dependency of CPS performance is to run several CPSs to create an ensemble, as in the AF experiment, which had the best skill in predicting the occurrence of rainfall in three out of six cases. Other studies (Du et al. 1997; Mullen and Buizza 2001; Grimit and Mass 2002) also show positive impacts to precipitation prediction by ensemble forecasting. Thus, *there may be some potential to improve rainfall-area prediction in the Taiwan area, by using an ensemble forecast with a mixture of several (four in this study) CPSs.*

In conclusion, quantitative precipitation forecasting in an operational model setting remains a very difficult task. There is no single cumulus scheme that consistently outperforms the others in all evaluation parameters of the rainfall forecast and across all weather systems (from cold-air outbreaks to summer thunderstorms, typhoons and Mei-Yu fronts). Finally, much work remains to be done to adequately understand how a CPS interacts with other components in a numerical weather prediction model, especially at mesoscale grid resolutions of 5–15 km.

Acknowledgements

This research is supported by the National Science Council in Taiwan under Grants NSC 91-2111-M-008-034, NSC 91-2625-Z-008-017, and NSC 91-2119-M-002-032. Use of the MM5 was made possible by the Microscale and Mesoscale Meteorological Division of NCAR. Satellite imagery and rain gauge data were provided by the Central Weather Bureau in Taiwan. Parts of the results were from the second author's M.S. thesis study. Special thanks go to Prof. Ching-Hwang Liu, Dr. Jen-Hsin Teng, and Mr. Shih-Ting Wang for their help on observation data, and Mr. Shih-Chieh Wang for computer graphics. Constructive criticism and suggestions by reviewers improved this paper substantially.

Appendix

The evaluation parameters

Some evaluation parameters used in this study are derived using a contingency table (Wilks 1995; Colle et al. 1999; Hamill 1999). This table represents a 2×2 matrix (Table A), where each element of the matrix holds the number of occurrences, in which the observations and the model did, or did not reach a certain threshold amount of precipitation for a given period of forecast (6 hours in this study). For example, if both the observation and the model verified at that point reach or exceed the threshold criteria, the number of occurrences in the "*A*" element in Table A is increased by one. Letters *A*, *B*, *C*, and *D* are used as in Wilks (1995) and Colle et al. (1999).

Table A. Rain contingency table used for verification. Each element of the matrix (*A*, *B*, *C*, and *D*) holds the number of occurrence in which the observations and/or the model forecasts reach a precipitation threshold amount for a given forecast period.

	Observed	
Forecasted	Rain	No rain
Rain	*A*	*B*
No rain	*C*	*D*

Based on this contingency table, one can calculate several evaluation parameters. The bias score (BS) is defined as

$$\mathrm{BS} = \frac{F}{O} = \frac{A+B}{A+C}, \tag{A1}$$

where F is the number of grid points where precipitation was forecasted to exceed a given threshold, and O is the number of observed grid points where rainfall exceeded the threshold. The equitable threat score (ETS) measures the skill in predicting a given threshold at a location and is defined as

$$\mathrm{ETS} = \frac{H-E}{F+O-H-E} = \frac{A-E}{A+B+C-E}, \tag{A2}$$

where H is the number of grid points where rainfall was correctly forecasted to exceed a given threshold (a "hit"), F and O are defined above, and the random-guess number E is defined as

$$E = \frac{FO}{N} = \frac{(A+B)(A+C)}{N}, \tag{A3}$$

where N is the total number of grid points verified ($A+B+C+D$). The ETS is similar to the threat score (TS),

$$\mathrm{TS} = \frac{H}{F+O-H} = \frac{A}{A+B+C}, \tag{A4}$$

except that the ETS corrects for the expected number of hit by chance (E).

In addition, an evaluation of rainfall-amount prediction was also performed using the following parameters. Mean error is defined as

$$\mathrm{ME} = \frac{1}{N}\sum_{n=1}^{N}(P_m - P_o)_n, \tag{A5}$$

where P_m and P_o are model, and observed precipitation on a grid point, respectively, and N is total number of grid points, where precipitation exceeds a threshold amount. A mean error percentage is defined as

$$\mathrm{MEP} = \frac{\mathrm{ME}}{\dfrac{1}{N}\displaystyle\sum_{n=1}^{N}(P_o)_n} \times 100\%, \tag{A6}$$

and a precipitation summary percentage is defined as

$$\mathrm{PSP} = \frac{\displaystyle\sum_{n=1}^{N}(P_{m06}+P_{m12}+P_{m18}+P_{m24}+P_{m30}+P_{m36})_n}{\displaystyle\sum_{n=1}^{N}(P_{o06}+P_{o12}+P_{o18}+P_{o24}+P_{o30}+P_{o36})_n} \times 100\%, \tag{A7}$$

where $P_{m06}, P_{m12}, P_{m18}, P_{m24}, P_{m30}, P_{m36}$ and $P_{o06}, P_{o12}, P_{o18}, P_{o24}, P_{o30}, P_{o36}$ are the model and observed rainfalls for each 6-h time period into simulation. Finally, a precipitation maximum percentage is defined as

$$\mathrm{PMP} = \frac{P_{M\,\max}}{P_{O\,\max}} \times 100\%, \tag{A8}$$

where $P_{M\,\max}, P_{O\,\max}$ are the model, and observed 6-h rainfall maximum, respectively.

References

Anthes, R.A., 1977: A cumulus parameterization scheme utilizing a one-dimensional cloud model. *Mon. Wea. Rev.*, **105**, 270–286.

Baldwin, M.E., J.S. Kain, and M.P. Kay, 2002: Properties of the convective scheme in NCEP's Eta model that affect forecast sounding interpretation. *Wea. Forecasting*, **17**, 1063–1079.

Betts, A.K. and M.J. Miller, 1986: A new convective adjustment scheme. Part II: Single column tests using GATE wave, BOMEX, ATEX, and Arctic air-mass data set. *J. Roy. Meteor. Soc.*, **112**, 693–709.

Blackadar, A.K., 1979: High resolution models of the planetary boundary layer. *Advances in Environmental Sciences and Engineering*, J. Pfafflin and E. Ziegler, Eds., Vol. 1, No. 1, Gordon and Breach, 50–85.

Chien, F.-C., Y.-H. Kuo, and M.-J. Yang, 2002: Precipitation forecast of MM5 in the Taiwan area during the 1998 Mei-yu season. *Wea. Forecasting*, **17**, 739–754.

Colle, B.A., K.J. Westrick, and C.F. Mass, 1999: Evaluation of MM5 and Eta-10 precipitation forecasts over the Pacific northwest during the cool season. *Wea. Forecasting*, **14**, 137–154.

Cressman, G.P., 1959: An operational objective analysis system. *Mon. Wea. Rev.*, **87**, 367–374.

Du, J., S.L. Mullen, and F. Sanders, 1997: Short-range ensemble forecasting for quantitative precipitation. *Mon. Wea. Rev.*, **125**, 2427–2459.

Dudhia, J., 1989: Numerical study of convection observed during the winter monsoon experiment using a mesoscale two-dimensional model. *J. Atmos. Sci.*, **46**, 3077–3107.

Gallus, W.A., Jr., 1999: Eta simulations of three extreme precipitation events: Sensitivity to resolution and convective parameterization. *Wea. Forecasting*, **14**, 405–426.

——— and M. Segal, 2001: Impact of improved initialization of mesoscale features on convective system rainfall in 10-km Eta simulations. *Wea. Forecasting*, **16**, 680–696.

Grell, G., 1993: Prognostic evaluation of assumptions used by cumulus parameterizations. *Mon. Wea. Rev.*, **121**, 764–787.

———, J. Dudhia, and D.R. Stauffer, 1994: A description of the fifth generation Penn State/NCAR Mesoscale Model (MM5). NCAR *Tech. Note NCAR/TN-398+STR*, 138 pp.

Grimit, E.P. and C.F. Mass, 2002: Initial results of a mesoscale short-range forecasting system over the Pacific northwest. *Wea. Forecasting*, **17**, 192–205.

Hamill, T.M., 1999: Hypothesis tests for evaluating numerical precipitation forecasts. *Wea. Forecasting*, **14**, 155–167.

Janjic, Z.I., 1994: The step-mountain eta coordinate model: Further developments of the convection, viscous sublayer, and turbulence closure schemes. *Mon. Wea. Rev.*, **122**, 927–945.

Kain, J.S. and J.M. Fritsch, 1993: Convective parameterization for mesoscale models: The Kain-Fritsch scheme. *The Representation of Cumulus Convection in Numerical Models*, *Meteor. Monogr.*, No. 46, Amer. Meteor. Soc., 165–177.

Kuo, Y.-H., R.J. Reed, and Y. Liu, 1996: The ERICA IOP 5 Storm. Part III: Mesoscale cyclogenesis and precipitation parameterization. *Mon. Wea. Rev.*, **124**, 1409–1434.

Liou, C.-S., J.-H. Chen, C.-T. Terng, F.-J. Wang, C.-T. Fong, T.E. Rosmond, H.-C. Kuo, C.-H. Shiao, and M.-D. Cheng, 1997: The second generation global forecast system at the Central Weather Bureau in Taiwan. *Wea. Forecasting*, **12**, 653–663.

McBride, J. and E.E. Ebert, 2000: Verification of quantitative precipitation forecasts from operational numerical weather prediction models over Australia. *Wea. Forecasting*, **15**, 103–121.

Mesinger, F., 1998: Comparison of quantitative precipitation forecasts by the 48- and by the 29-km Eta model: An update and possible implications. Preprint, *12th Conf. on Numerical Weather Prediction*, Phoenix, AZ, Amer. Meteor. Soc., J22–J23.

Mullen, S.L. and R. Buizza, 2001: Quantitative precipitation forecasts over the United States by the ECMWF ensemble prediction system. *Mon. Wea. Rev.*, **129**, 638–663.

Peng, X. and K. Tsuboki, 1997: Impact of convective parameterizations on mesoscale precipitation associated with the Baiu front. *J. Meteor. Soc. Japan*, **75**, 1141–1154.

Rogers, R.F. and J.M. Fritsch, 1996: A general framework for convective trigger function. *Mon. Wea. Rev.*, **124**, 2438–2452.

Spencer, P.L. and D.J. Stensrud, 1998: Simulating flash flood events: Importance of the subgrid representation of convection. *Mon. Wea. Rev.*, **126**, 2884–2912.

Stensrud, D.J., J.-W. Bao, and T.T. Warner, 2000: Using initial condition and model physics perturbations in short-range ensemble simulations of mesoscale convective systems. *Mon. Wea. Rev.*, **128**, 2077–2107.

Wang, W. and N.L. Seaman, 1997: A comparison study of convective parameterization schemes in a mesoscale model. *Mon. Wea. Rev.*, **125**, 252–278.

Wilks, D.S., 1995: *Statistical Methods in the Atmospheric Sciences*. Academic Press, 467 pp.

Yang, M.-J., F.-C. Chien, and M.-D. Cheng, 2000: Precipitation parameterizations in a simulated Mei-Yu front. *Terr., Atmos. and Oceanic Sci.*, **11**, 393–422.

Zhang, D.-L. and R.A. Anthes, 1982: A high-resolution model of the planetary-boundary layer—Sensitivity tests and comparisons with SESAME-79 data. *J. Appl. Meteor.*, **21**, 1594–1609.